Protocol to study wavefront preservation capabilities of reflective X-ray optics with coherent synchrotron light

NIMA_PROCEEDINGS-D-12-00316 Rev1

A. Rack

European Synchrotron Radiation Facility, BP 220, 38043 Grenoble, France, email: arack@snafu.de

T. Weitkamp

Synchrotron Soleil, BP 48, 91192 Gif-sur-Yvette, France

L. Assoufid

Advanced Photon Source, Argonne National Laboratory, Argonne, Illinois, USA

T. Rack

Charité, Campus Virchow Clinic, 13353 Berlin, Germany

I. Zanette, Ch. Morawe, R. Kluender

European Synchrotron Radiation Facility, BP 220, 38043 Grenoble, France

C. David

Paul Scherrer Institut, 5232 Villigen-PSI, Switzerland, email: christian.david@psi.ch

Abstract

Wavefront preservation of reflective X-ray optics, i. e., homogeneity and coherence properties of the reflected beam, are of crucial importance for their application in combination with high-brilliance synchrotron light sources. In order to compare the performance of optical elements in a quantitative manner, a protocol has been established using the Talbot effect to access the coherence properties of the reflective beam as well as long propagation distance imaging to study its homogeneity. The basic idea is to operate in a single-bounce geometry: a high-resolution imaging detector translated at short propagation distances along the beam is used to measure the visibility of a diffraction grating in transmission geometry placed close to the mirror under study. The change of the fringe visibility as a function of distance between the grating and the detector gives access to the angular source size. A second high-resolution imaging detector at longer propagation distances of up to several meters allows one to measure the homogeneity of the beam. This article outlines the concept as realized at beamline ID19 of the European Synchrotron Radiation Facility, gives insight into some of the technical details to be considered for implementation at other facilities and ends with an example application: the study of a W/B_4C multilayer mirror.

Keywords: X-ray optics, multilayer mirrors, X-rays, coherence, X-ray monochromators, X-ray imaging, X-ray phase contrast, Talbot effect, synchrotron radiation

1. Introduction

Reflective optics are widely used in combination with hard X-rays, e. g., Bragg-reflection on single-crystals or reflection on flat multilayer mirrors for monochromatization purposes,

or total reflection on (single-coated) X-ray mirrors to suppress higher harmonics for example of an undulator source [1]. Recently, reflection on curved multilayer-coated KB-mirrors has been successfully used to reach sub-100 nm focusing of hard X-rays [2].

However, as any optical element, reflective X-ray optics show deviations from their ideal behavior. These deviations originate from various sources, such as roughness or slope errors of reflective surfaces and interfaces, effects of dynamical diffraction (in the case of crystal optics), contamination of the surfaces, etc., and they can affect any of the performance parameters of the devices, e. g., the homogeneity (flatness) of the beam profile at the sample position, the smoothness of the wavefront phase profile, and the coherence properties of the beam.

An example of wavefront modification caused by a reflective optical element is the beam profile after reflection on a multilayer mirror [3]. Commonly, this reflected beam profile shows a typical stripe modulation in combination with a certain loss of coherence properties. Such degradation of the wavefront can be detrimental for phase-sensitive imaging techniques [4], [5], [6]. Attempts to improve the wavefront preservation capability of multilayer mirrors require quantitative approaches to characterize the degradation of the wavefront due to reflection on such mirrors.

This article will introduce a protocol which has recently been established to compare multilayer mirrors consisting of different material compositions [3], [8], [9], or that were made by varying coating parameters [10], or using different coating facilities [11] at beamlines 32-ID (Advanced Photon Source APS, USA) as well as ID06 and ID19 (European Synchrotron Radiation Facility ESRF, France). The basic idea is to measure at short propagation distances the visibility of a phase grating which is placed close to the reflective optical element. The change of the visibility at different Talbot distances gives access to the vertical and horizontal angular source size [12], [13]. At larger propagation distances, modifications of the wavefront are transformed into intensity modulations and hence, allow one to depict the homogeneity of the reflected beam [14]. Besides the technical details of the implementation, a few issues worth considering when implementing the protocol at other facilities are described together with an example application.

2. Experiment

The experimental setup as used at beamline ID19 of the ESRF is depicted in Figure 1 [15]. Optics characterization studies are commonly performed at ID19 with the storage ring operating in the so-called 4-bunch mode, because of beamtime availability issues. In this mode the storage ring electron current is 40 mA, i. e., only 20% of the maximum user-mode value. The two U32 undulator insertion devices of the beamline are combined in order to achieve a sufficient photon flux density. A diamond window placed close to the front-end is used to suppress the softer part of the spectrum. The vertical reflecting double-crystal monochromator 140 m downstream of the source is applied to select a wavelength of 18 keV to illuminate the optical element under study. The photon energy is selected as by experience a majority of high-resolution X-ray imaging experiments using synchrotron light are performed using energies from a range around this value. Illuminating with a well-defined energy subsequently reduces the alignment effort, i. e. it is sufficient to rock the reflective optics while tracking the reflected beam with a large phosphor screen and a video camera. Furthermore, the heat load downstream of the crystal monochronmator is negligible, allowing one to mount the optics under test in air without further cooling. In this configuration, the degradation of the wavefront with respect to the beam as only reflected by the silicon crystals of the monochromator is measured.

The mount for the optical element is shown in Figure 2. A simple aluminium plate is used as a base, bars are located upstream and downstream of the element in a shiftable manner. They can be tightened to the plate for fixation of the optics without introducing mechanical stress. The mount is fixed on a double-cradle system (Huber Diffraktionstechnik GmbH & Co. KG, Germany) in order to correct the roll and chose the angle of incidence. This

setting is then mounted on the sample manipulator of the high-resolution tomograph of the ID19 beamline. The manipulator is used to align the reflective optics with respect to the incoming beam.

A phase grating is positioned downstream of the optics (typically approximately 10 cm away) on translation stages to align the grating with respect to the beam and move it out of the beam for taking reference images, cf. Figure 2. The high-resolution tomograph is additionally equipped with a 1 m high-precision linear axis in order to translate an X-ray detector along the beam (frequently used in combination with holotomography [4]). Due to the fact that ID19 operates a single-bounce vertically deflecting multilayer as monochromator as well, the entire tomograph including the detector axis can be tilted by several degrees around a horizontal transverse axis; the detector translation can thus be aligned to move parallel to a beam reflected upward by a multilayer. This configuration is used to measure the visibility of the phase grating at different distances. On instruments without a tiltable stage, the detector can be translated along the beam by adding another linear stage for vertical translation [11]. A second high-resolution detector is positioned further downstream; in the case of ID19 it is located on the medium-resolution tomograph, 6.1 m from the reflective optics tested.

In order to study the coherence properties by means of Talbot imaging, it is beneficial to operate with shorter propagation distances between the grating and the first imaging detector and with the grating close to the optical element: the visibility of the phase grating in the images is determined by the coherence of the impinging wavefront but image analysis is also affected by the accuracy of the flat-field correction [6]. Simply speaking: measuring the coherence properties close to the reflective optical element allows one to work with a rather homogeneous beam profile and hence, suppresses unwanted artifacts due to imperfect flat-field corrections [7]. Furthermore, the influence of potential angular instabilities of the investigated optical element is reduced. Commonly, the visibility is scanned starting from a propagation distance around zero to the second Talbot distance in equidistant steps that are much smaller than the Talbot distance. Compared to measuring only at the Talbot distances (i. e., the visibility maxima), this increases to a certain degree the sensitivity of the characterization. For example, focusing effects can shift the maximum visibility away from the Talbot distance (see as well Section 5.2). In order to measure the homogeneity of the reflected wavefront, a second detector is positioned several meters downstream (with the phase grating and first detector out of the beam). Phase distortions introduced to the wavefront due to the reflection on, e. g. an imperfect surface are converted into intensity modulations due to the long propagation of the beam [14], [16].

3. Phase Grating

The test object was made from a 0.25-mm-thick silicon ⟨100⟩ substrate. The grating pattern, a mesh of square dots on a Cartesian grid, was exposed into a resist layer of polymethyl methacrylate (PMMA) using a Vistec EBPG 5000 plus electron-beam lithography system (Vistec Electron Beam GmbH, Jena, Germany) at 100 keV electron energy [17]. After development the resist pattern was transferred into a 25-nm-thick chromium layer by dry etching in a Cl_2/CO_2 plasma [18]. This layer served as a hard mask for the pattern transfer into the silicon substrate using a reactive ion etching process in a SF_6/C_4F_8 plasma. The resulting structures are 5 µm deep and have nearly vertical side walls, cf. Figure 3. At a photon energy of 18 keV, this corresponds to a phase shift of 0.68 rad (i. e., $\approx \pi/5$), while the absorption in the structures remains negligible (0.6%).

4. Data Processing

For the data processing, an ESRF inhouse developed code is applied which has already been described in detail elsewhere [19]. The approach of first integrating the image of

the phase grating horizontally and vertically in order to achieve line profiles of the intensity, with a reduced noise level compared to individual section profiles, was found to be very robust under different experimental conditions [9], [11]. The visibility is then determined by Fourier analysis. Alternative processing concepts, in which the visibility is first calculated locally and then the mean over all visibility values is determined, or using a two-dimensional Fourier transform, were found to be more sensitive to noise.

5. Considerations

A few issues frequently appear when studying the wavefront preservation capabilities by means of Talbot imaging and long propagation distance imaging. For the reader who is interested in implementing the protocol described in this article, the major issues which can occur are briefly described below.

5.1. Storage Ring

The measured visibility of the phase grating can vary drastically during and after a machine refill (i. e. the storage ring is not operated in top-up mode). An extreme example is shown in Figure 4 (top) where a refill occurred during a visibility scan (the storage ring operated in the so-called 4-bunch mode). The inset shows the approximated visibility plot before and after the refill, the visibility drops significantly from 0.25 to 0.20 due to the refill.

5.2. Wavefront curvature

The data processing approach as described in Section 4 is strictly valid only in case of a parallel beam. The finite distance to the source, as well as any focusing effects induced by beamline optics or the element tested cause deviations from this condition. A divergent beam magnifies the image for larger propagation distances and hence, artificially increases the size of the grating structures as projected onto the detector. Frequently, the modulation-transfer function of the detectors used increases for lower frequencies, i. e. the enlarged image determines an artificially increased visibility. The effect of the distance from the source and of focusing beamline optics with known focal lengths can be corrected. However, in the case of strongly bent reflecting optics which diverge or focus the beam, the protocol described in this article will not deliver correct results.

5.3. Detector

The indirect high-resolution detectors commonly used are based on visible light microscopy combined with scintillator screens [20]. The spatial resolution of a visible light microscope drops from the center of the image towards the border. This can affect as well the measured visibility as shown in Figure 4 (bottom): regions-of-interest (ROI) of an grating image at a fixed propagation distance were analyzed. The ROIs were chosen along a horizontal line in the middle of the field-of-view. The analyzed ROI should therefore be chosen as close as possible to the center of the field-of-view. Furthermore, the ROI should be kept the same at least during one measurement campaign.

5.4. Reproducibility

Due to the aspects mentioned in the previous three sections, it is recommended to have a calibration sample which is measured during each individual measurement campaign. By doing so, results from different campaigns are comparable to a certain degree, i. e. the reproducibility of the results is verified.

6. Example

W-based multilayer mirrors are frequently used for monochromatization in combination with hard X-ray imaging at synchrotron beamlines, e. g., TOMCAT at the Swiss Light Source [21], BAM*line* at BESSY-II, Germany [22], TopoTomo at ANKA, Germany [23], 2-BM of the APS, USA [24], or ID19 at the ESRF, France [15]. Here we present measurements on a W/B_4C multilayer mirror produced by means of magnetron sputtering at the ESRF multilayer deposition laboratory [25]. The multilayer consists of 120 bilayers with a period (*d* spacing) of 2 nm, which have been deposited on a Si substrate (General Optics, USA, 100 mm × 20 mm × 18 mm). The ratio Γ between the thickness of each W layer and the bilayer period *d* was set to a nominal value of 0.5. Further details on the coating parameters have already been reported [10, 11].

The experiment was carried out at the ESRF beamline ID19 as described above. The multilayer was illuminated with photons of 18 keV energy. A phase grating with a pitch of 6 μm was used. The first detector operated with 0.70 μm effective pixel size (10× objective with 0.3NA combined with a 2× eye-piece), a scan of the visibility was performed for propagation distances ranging from 100 mm to 840 mm. The second detector at 6.1 m fixed propagation distance operated with an effective pixel size of 0.75 μm (10× objective with 0.3NA combined with a 2× eye-piece). The results are depicted in Figure 5. The angular source size as derived from the visibility at the two given Talbot distances is: 1.54 μrad (horizontal) × 1.69 μrad (vertical) (without multilayer reflection: 1.48 μrad × 1.28 μrad). As can be expected, the horizontal source size remained rather unchanged while the vertical source size is affected by the vertically deflecting multilayer mirror. The picture of the beam profile in Figure 5 has been normalised to the mean gray-value. The profile plot reveals a rather strong modification with respect to the flat incoming beam with peak-to-valley values of up to 50%.

7. Summary

A protocol to study wavefront preservation capabilities of reflective X-ray optics has been described. It is relatively simple to implement into existing imaging instruments at a synchrotron beamline. While the beamline ID19 of the ESRF is specially well-suited for this kind of studies due to its coherence properties, the long experimental hutch and the tiltable high-precision linear stage for the detector, the protocol has already been successfully applied at other stations such as 32-ID (APS) and ID06 (ESRF) as well [10], [11], [19].

The characterization of optical elements in transmission mode is possible with this protocol, as long as these elements do not substantially change the wavefront curvature (cf. Section 5.2). So far, single crystal Be windows were studied [26].

Acknowledgments

We would like to thank Jean-Paul Valade (ESRF) for the design and construction of the multilayer mount and for technical support during various experiments. Vitaliy Guzenko and Christian Spreu (PSI) made the gratings, for which they are gratefully acknowledged. T. W. received support from the French research networks (RTRA) “Digiteo” and “Triangle de la Physique” (grants 2009-034T and 2009-79D). Work performed at Argonne was supported by the UChicago Argonne, LLC, operator of Argonne National Laboratory (”Argonne”). Argonne, a U.S. Department of Energy Office of Science laboratory, was operated under contract No. DE-AC02-06CH11357.

References

[1] W. Graeff, K. Engelke, Microradiography and Microtomography, in: S. Ebashi, M. Koch, E. Rubenstein (Eds.), Handbook on Synchrotron Radiation, Vol. 4, North-Holland; Amsterdam, Oxford, New York, Tokyo, 1991, pp. 361–406.

[2] G. Martínez-Criado, R. Tucoulou, P. Cloetens, P. Bleuet, S. Bohic, J. Cauzid, I. Kieffer, E. Kosior, S. Labouré, S. Petitgirard, A. Rack, J. A. Sans, J. Segura-Ruiz, H. Suhonen, J. Susini, J. Villanova, Status of the hard X-ray microprobe beamline ID22 of the European Synchrotron Radiation Facility, J. Synchrotron Radiat. 19 (1) (2012) 10–18. doi:10.1107/S090904951104249X.

[3] A. Rack, T. Weitkamp, M. Riotte, D. Grigoriev, T. Rack, L. Helfen, T. Baumbach, R. Dietsch, T. Holz, M. Krämer, F. Siewert, M. Meduňa, P. Cloetens, E. Ziegler, Comparative study of multilayers used in monochromators for synchrotron-based coherent hard x-ray imaging, J. Synchrotron Radiat. 17 (4) (2010) 496–510.

[4] P. Cloetens, W. Ludwig, J. Baruchel, D. V. Dyck, J. Landuyt, J. P. Guigay, M. Schlenker, Holotomography: Quantitative phase tomography with micrometer resolution using hard synchrotron radiation X-rays, Appl. Phys. Lett. 75 (1999) 2912–2914.

[5] D. Paganin, S. C. Mayo, T. E. Gureyev, P. R. Miller, S. W. Wilkins, Simultaneous phase and amplitude extraction from a single defocused image of a homogeneous object, J. Microsc. 206 (2002) 33–40. doi:10.1046/j.1365-2818.2002.01010.x.

[6] T. Weitkamp, D. Haas, D. Wegrzynek, A. Rack, ANKAphase: software for single-distance phase retrieval from inline X-ray phase-contrast radiographs, J. Synchrotron Radiat. 18 (4) (2011) 617–629. doi:10.1107/S0909049511002895.

[7] J. I. Espeso, P. Cloetens, J. Baruchel, J. Härtwig, T. Mairs, J.-C. Biasci, G. Marot, M. Salomé-Pateyron, M. Schlenker, Conserving the coherence and uniformity of third-generation synchrotron radiation beams: the case of ID19, a 'long' beamline at the ESRF, J. Synchrotron Radiat. 5 (5) (1998) 1243–1249. doi:10.1107/S0909049598002271.

[8] A. Rack, T. Weitkamp, I. Zanette, C. Morawe, A. V. Rommeveaux, P. Tafforeau, P. Cloetens, E. Ziegler, T. Rack, A. Cecilia, P. Vagovič, E. Harmann, R. Dietsch, H. Riesemeier, Coherence preservation and beam flatness of a single-bounce multilayer monochromator (beamline ID19 – ESRF), Nucl. Instr. & Meth. in Phys. Res. A 649 (1) (2011) 123–127, Proceedings of the 16th Pan-American Synchrotron Radiation Instrumentation Conference (SRI2010). doi:10.1016/j.nima.2010.11.069.

[9] A. Rack, L. Assoufid, R. Dietsch, T. Weitkamp, S. B. Trabelsi, T. Rack, F. Siewert, M. Krämer, T. Holz, I. Zanette, W.-K. Lee, P. Cloetens, E. Ziegler, Study of multilayer-reflected beam profiles and their coherence properties using beamlines ID19 (ESRF) and 32-ID (APS), Vol. 1437 of AIP Conference Proceedings (ICXOM21), AIP, 2012, pp. 15–17.

[10] C. Morawe, R. Barrett, K. Friedrich, R. Klünder, A. Vivo, Spatial coherence studies on x-ray multilayers, in: S. G. Ch. Morawe, A. M. Khounsary (Ed.), Advances in X-Ray/EUV Optics and Components VI, Vol. 8139 of Proc. of SPIE, SPIE, 2011, p. 813909. doi:10.1117/12.894617.

[11] A. Rack, L. Assoufid, W.-K. Lee, B. Shi, C. Liu, C. Morawe, R. Kluender, R. Conley, N. Bouet, Hard X-ray multilayer mirror round-robin on the wavefront preservation capabilities of W/B_4C coatings, Rad. Phys. Chem. 81 (11) (2012) 1696–1702. doi:10.1016/j.radphyschem.2012.06.015.

[12] P. Cloetens, J. P. Guigay, C. De Martino, J. Baruchel, M. Schlenker, Fractional Talbot imaging of phase gratings with hard x rays, Opt. Lett. 22 (14) (1997) 1059–1061. doi:10.1364/OL.22.001059.

[13] J.-P. Guigay, S. Zabler, P. Cloetens, C. David, R. Mokso, M. Schlenker, The partial Talbot effect and its use in measuring the coherence of synchrotron X-rays, J. Synchrotron Radiat. 11 (6) (2004) 476–482.

[14] P. Cloetens, R. Barrett, J. Baruchel, J.-P. Guigay, M. Schlenker, Phase objects in synchrotron radiation hard x-ray imaging, J. Phys. D: Appl. Phys. 29 (1) (1996) 133–146.

[15] T. Weitkamp, P. Tafforeau, E. Boller, P. Cloetens, J.-P. Valade, P. Bernard, F. Peyrin, W. Ludwig, L. Helfen, J. Baruchel, Status and evolution of the ESRF beamline ID19, Vol. 1221 of AIP Conf. Proc. (ICXOM20), 2010, pp. 33–38. doi:10.1063/1.3399253.

[16] A. Snigirev, I. Snigireva, V. Kohn, S. Kuznetsov, I. Schelokov, On the possibilities of x-ray phase contrast microimaging by coherent high-energy synchrotron radiation, Rev. Sci. Instrum. 66 (12) (1995) 5486–5492. doi:10.1063/1.1146073.

[17] V. A. Guzenko, J. Romijn, J. Vila-Comamala, S. Gorelick, C. David, Efficient e-beam lithography exposure strategies for diffractive x-ray optics, AIP Conf. Proc. 1365 (2011) 92–95.

[18] C. David, D. Hambach, Line width control using a defocused low voltage electron beam, Microelectron. Eng. 46 (1–4) (1999) 219–222. doi:10.1016/S0167-9317(99)00066-0.

[19] R. Kluender, F. Masiello, P. van Vaerenbergh, J. Härtwig, Measurement of the spatial coherence of synchrotron beams using the Talbot effect, Phys. Status Solidi A 206 (8) (2009) 1842–1845.

[20] A. Koch, C. Raven, P. Spanne, A. Snigirev, X-ray imaging with submicrometer resolution employing transparent luminescent screens, J. Opt. Soc. Am. 15 (1998) 1940–1951.

[21] M. Stampanoni, A. Groso, A. Isenegger, G. Mikuljan, Q. Chen, D. Meister, M. Lange, R. Betemps, S. Henein, R. Abela, TOMCAT: A beamline for TOmographic Microscopy and Coherent rAdiology experiments, in: J.-Y. Choi, S. Rah (Eds.), AIP Conference Proceedings (SRI2006), Vol. 879, 2007, pp. 848–851.

[22] A. Rack, S. Zabler, B. R. Müller, H. Riesemeier, G. Weidemann, A. Lange, J. Goebbels, M. Hentschel, W. Görner, High resolution synchrotron-based radiography and tomography using hard X-rays at the BAMline (BESSY II), Nucl. Instr. & Meth. in Phys. Res. A 586 (2) (2008) 327–344.

[23] A. Rack, T. Weitkamp, S. Bauer Trabelsi, P. Modregger, A. Cecilia, T. dos Santos Rolo, T. Rack, D. Haas, R. Simon, R. Heldele, M. Schulz, B. Mayzel, A. N. Danilewsky, T. Waterstradt, W. Diete, H. Riesemeier, B. R. Müller, T. Baumbach, The micro-imaging station of the TopoTomo beamline at the ANKA synchrotron light source, Nucl. Instr. & Meth. in Phys. Res. B 267 (11) (2009) 1978–1988. doi:10.1016/j.nimb.2009.04.002.

[24] Y. S. Chu, C. Liu, D. C. Mancini, F. De Carlo, A. T. Macrander, B. Lai, D. Shu, Performance of a double-multilayer monochromator at Beamline 2-BM at the Advanced Photon Source, Rev. Sci. Instrum. 73 (3) (2002) 1485–1487. doi:10.1063/1.1423628.

[25] C. Morawe, C. Borel, J.-C. Peffen, The new ESRF multilayer deposition facility, in: A. M. Khounsary, C. Morawe, S. Goto (Eds.), Advances in X-Ray/EUV Optics and Components II, Vol. 6705 of Proc. of SPIE, 2007, p. 670504. doi:10.1117/12.734107.

[26] A. Khounsary, B. Lai, A. Rack, S. Goto, O. Chubar, T. Weitkamp, Progress on single crystal beryllium windows, in: S. G. Ch. Morawe, A. M. Khounsary (Ed.), Advances in X-Ray/EUV Optics and Components VI, Vol. 8139 of Proc. of SPIE, SPIE, 2011, p. 813914. doi:10.1117/12.895391.

Figures

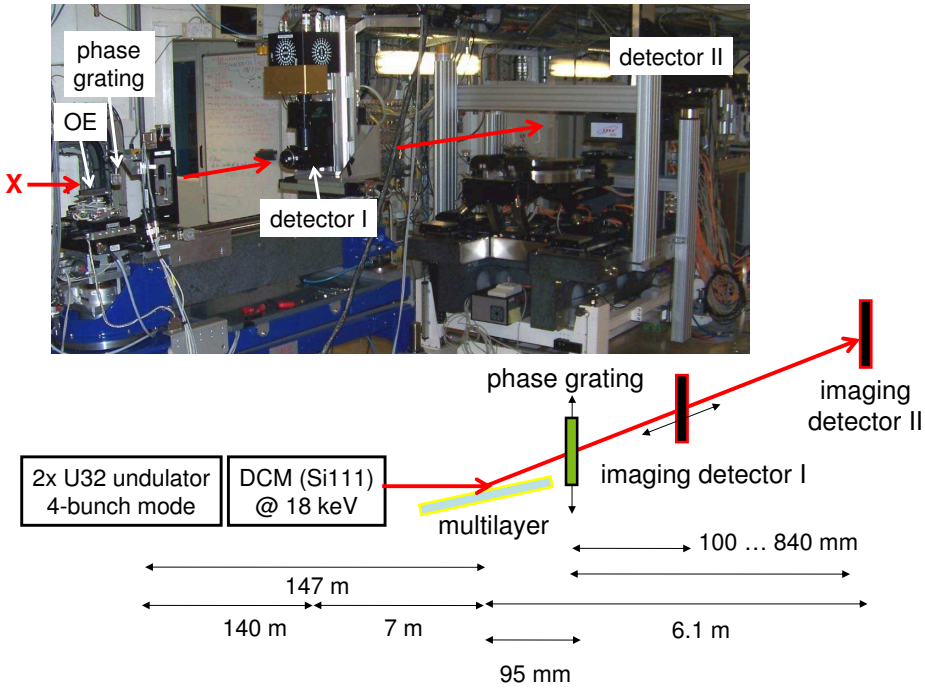

Figure 1: [2-column-span, color online only] The experimental setup as typically used at ID19, the inset shows a photo of the experimental hutch [15]. The reflective optical element (OE) is mounted on the so-called high-resolution tomograph, its detector can be translated along the beam over a travel range of 1 m. A second detector at the end of the hutch is used to grab a picture of the beam profile. Details of the mount for the optical element under study are shown in Figure 2.

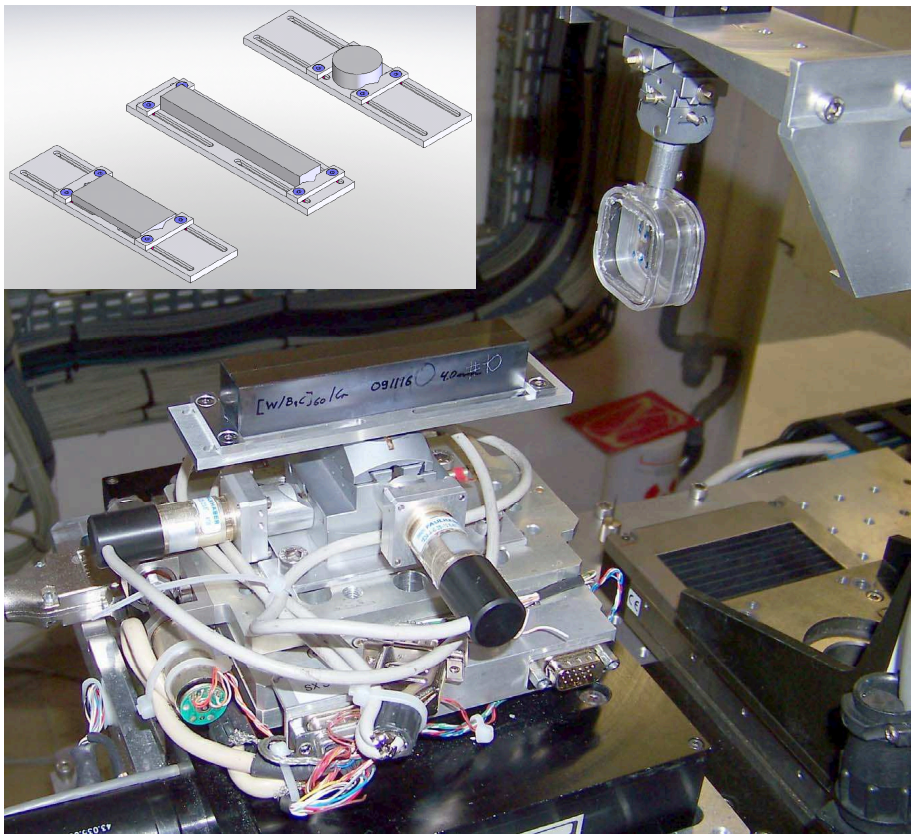

Figure 2: [1-column-span, color online only] The mount for the optical element (here shown with a multilayer mirror in the center of the picture): an aluminium plate with shiftable bars which can be tightened in order to fix the element without introducing mechanical stress. Below a double-cradle system to align the roll as well as to chose the incidence angle. The inset shows a sketch of the mount for different substrate geometries. In the upper right part of the image, the phase grating can be seen, mounted in a protective box on a diffractometer head as well as on horizontal and vertical translation stages.

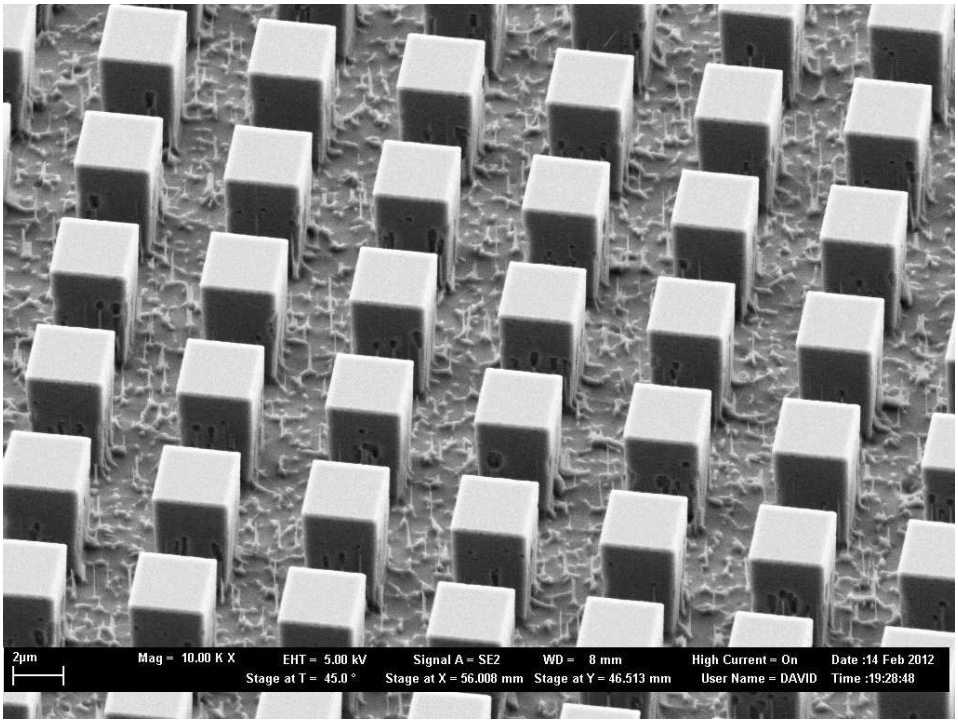

Figure 3: [1-column-span] Scanning-electron microscopy of the phase-grating used as test pattern to measure the coherence properties of the reflected beam.

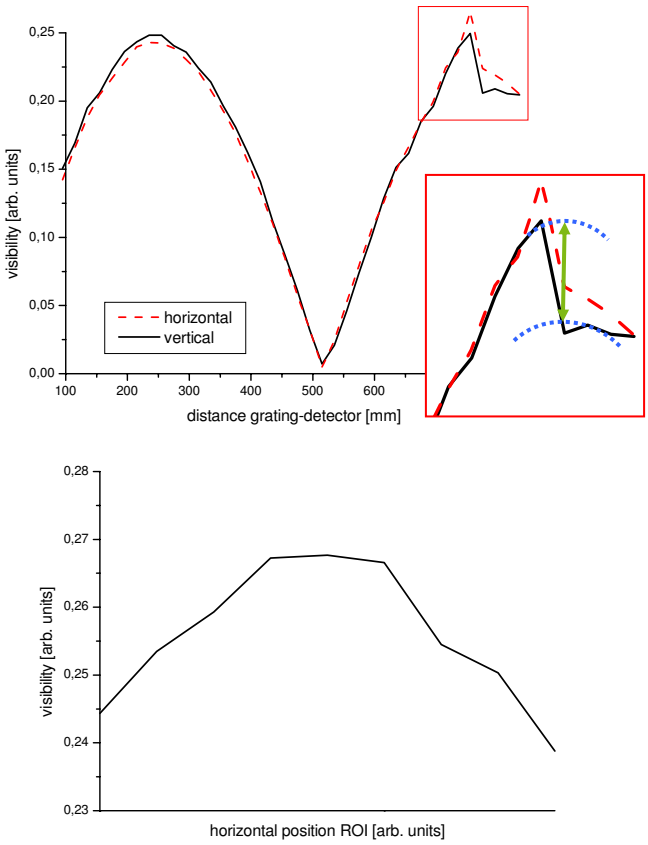

Figure 4: [1-column-span, color online only] Top: change of the visibility during a scan due to a refill marked in red (red box with zoomed inset: dotted lines depict the approximated curves, the arrow marks the absolute drop in intensity). Bottom: variation of the measured visibility due to different regions-of-interest selected along the middle horizontal line of the field-of-view of the deployed indirect detector.

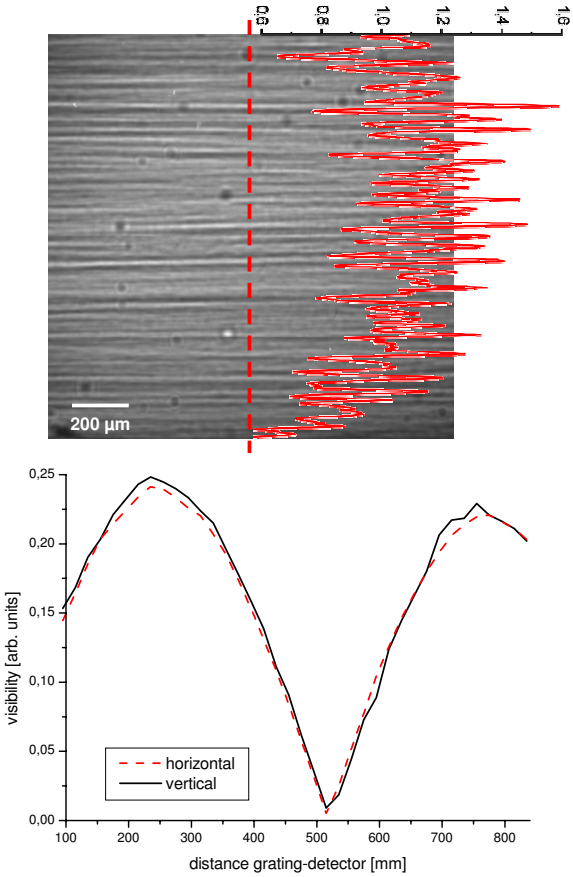

Figure 5: [1-column-span, color online only] Results of the characterization of a W/B_4C multilayer mirror (2.0 nm *d* spacing, 120 bilayers, ESRF multilayer laboratory). Top: the beam profile after 6.1 m of propagation. A profile plot of the marked line (normalised to the mean gray-value of the image) is used as a measure of the intensity modulation. Bottom: plot of the horizontal and vertical visibility of the phase grating measured at different propagation distances. The respective angular source sizes as derived from the two Talbot distances given are: 1.54 µrad (horizontal) × 1.69 µrad (vertical).